Exp Brain Res (1988) 71: 189–198

Experimental Brain Research

Cell dynamics in the olfactory epithelium of the tiger salamander: a morphometric analysis

A. Mackay-Sim[1], W. Breipohl[2], and M. Kremer[3]

[1] Department of Physiology, University of Adelaide, Adelaide, S.A. 5000, Australia
[2] Department of Anatomy, University of Queensland, St. Lucia, QLD 4067, Australia
[3] Institut für Anatomie der Universität Essen, Hufelandstraße 55, D-4300 Essen 1, Federal Republic of Germany

Summary. The factors controlling neurogenesis and differentiation of olfactory receptor cells in adults are poorly understood, although it is often stated that these cells undergo continual turnover after a predetermined lifespan. An interesting model in which to study mechanisms which control olfactory receptor neurogenesis and cell turnover is the tiger salamander, since basal cell mitosis varies with epithelial thickness and location in the nasal cavity. This paper presents a quantitative light-microscopic study of the different cell types within the ventral olfactory epithelium of the tiger salamander using a computer-assisted morphometric analysis of 2 μm sections. The results show that the surface density of olfactory vesicles remained constant throughout most of the epithelium and was independent of nasal cavity location, epithelial thickness and the total number of nuclei per unit epithelial surface area. Histological classification of nuclei into different cell types indicated that the increase in total cell number with epithelial thickness was mainly due to an increase in the number of immature receptor cells since the number of supporting cells varied only slightly and the numbers of basal cells and mature receptor cells remained constant except in the thinnest, most caudally located epithelium. It is concluded that the rate of maturation of receptor cells may be limited by an optimal surface density of olfactory vesicles. That is, when this density reaches 4.5×10^4 vesicles per mm^2 there is a physical or chemical mechanism which prevents the final maturation of newly developing receptor cells, leading to their accumulation. This mechanism may also account for the variations in basal cell mitosis in this species.

Key words: Neurogenesis – Neural development – Olfactory receptor cell – Tiger salamander

Offprint requests to: A. Mackay-Sim, School of Science, Griffith University, Nathan, QLD 4111, Australia

Introduction

Whilst the technique of ^{3}H-thymidine autoradiography would seem to be well suited to observe the dynamic process of neurogenesis it is now apparent that there are some shortcomings in this method as applied to neurogenesis in the adult olfactory epithelium (Breipohl et al. 1985a, b). Certainly it is known that thymidine is incorporated into nuclei during division of neuronal progenitor cells in the basal cell layer of the olfactory epithelium and that the daughter cell nuclei, labelled with ^{3}H-thymidine, migrate into the receptor cell layer (Moulton et al. 1970; Graziadei and Metcalf 1971; Graziadei and Monti Graziadei 1979; Mackay-Sim and Patel 1984). A problem with these studies is in the assumption that migration of a nucleus into the receptor cell layer is followed by full maturation of the cell, with the growth of a dendrite to the epithelial surface and an axon to the olfactory bulb. As recently emphasised, current ^{3}H-thymidine evidence for turnover of mature olfactory receptor cells can also be interpreted as evidence for turnover of immature elements, with mature cells remaining in place for many months (Hinds et al. 1984). This turnover of immature receptor cells may be accelerated by hypothyroidism (Mackay-Sim and Beard 1987). In hypothyroid mice 75% of labelled nuclei were lost between 5 and 15 days after ^{3}H-thymidine injection. Paradoxically, despite 50 days of anti-thyroid treatment, and the loss of immature receptor cells, the hypothyroid mice still had mature receptor cells as indicated by the size and number of glomeruli in the olfactory bulb, and the presence of marker protein in the epithelium, nerve and bulb (Mackay-Sim and Beard 1987).

A curious property of the tiger salamander olfactory epithelium has led us to re-examine the dynamic process of olfactory neurogenesis through the "sta-

tic" technique of morphometry. In this study the variable is not time but epithelial thickness which, in this species, increases linearly from caudal to rostral in the nasal cavity (Mackay-Sim and Patel 1984). Since the major factor in epithelial thickness is the number of cells, it is of interest to know the identity of the cells which contribute to the increasing epithelial thickness, particularly when it is realised that after ^{3}H-thymidine injection there is an inverse relation between epithelial thickness and the number of labelled nuclei (Mackay-Sim and Patel 1984). This latter observation indicates that basal cell mitosis varies with epithelial thickness, and raises the possibility that the rate of turnover of immature or mature receptor cells also varies.

The aim of the present study is to investigate the relation between rostro-caudal variations in epithelial thickness and the numbers of basal, receptor and supporting cells within sections that represent a standardised area of epithelial surface. Of special interest in this study are the numbers of mature and immature receptor cells, the former being those with an olfactory vesicle at the epithelial lumen.

Methods

Epithelial area

Thirty four wild-caught, land-phase tiger salamanders (*Ambystoma tigrinum*) were obtained from Amphibians of North America (Nashville, TN). The weight of these animals was 56.62 ± 0.26 g (mean ± SEM). They were anaesthetized by immersion in an ice bath, pithed, and the ventral surface of their nasal cavities was surgically exposed and photographed through the dissection microscope at 10 × magnification. The animals used here were used previously for electrophysiological studies of the olfactory epithelium (Mackay-Sim et al. 1982; Mackay-Sim and Shaman 1984).

The area of each epithelium was measured from the photograph using a computerised morphometry program run on an Apple IIe computer with a video input (Halasz and Martin 1984).

Counts of cell nuclei and olfactory vesicles

Three animals were used for the morphometric histological study. These were killed by cervical decapitation and their olfactory chambers were perfused with 3.2% glutaraldehyde and 2.6% paraformaldehyde in cacodylate buffer (0.09 M; pH 7.3). The heads were kept in this solution for several hours to several days at 4° C. After saline washing a 5 mm rostro-caudal strip from the ventral surface of the olfactory epithelium was dissected and processed as described previously (Breipohl et al. 1973).

Each piece of epithelium was sectioned transversally, in serial order, every 2 μm over a total distance of about 4–5 mm. Six sections, each 72 μm apart, were selected for analysis at every 1 mm along the rostro-caudal length of the epithelium. This gave about 30 sections per animal.

On each section, cell nuclei were counted in a field width of 200 μm along the epithelial surface. All counts were made at a magnification of 600 × using a computerised morphometry program run on an Apple IIe computer (Halasz and Martin 1984). Briefly, a "mouse" attachment for the computer is used to input data and register counted cells on the computer monitor screen which is viewed through the camera lucida attachment of the microscope. Thus, the screen image of cells counted appears superimposed on the microscope image of the same cells. In this way about 6000 cell nuclei and about 600 olfactory vesicles were counted for each animal. Different cell types were identified as usual by their location within the epithelium, and by the different shapes and staining characteristics of their nuclei (Graziadei and Monti Graziadei 1976).

Profile diameters

Using the same computer program, the diameters of 450 nuclei and 75 olfactory vesicles were measured parallel to the lumenal surface at 1250 × magnification, under oil immersion. The average diameter of the supporting cell cytoplasm at the lumenal surface was also measured at this magnification from sections of epithelium throughout the nasal cavity.

Since the section thickness was small (2 μm) compared to the average diameters of the nuclei and the supporting cell lumenal surface these were multiplied by $4/\pi$ to give the "true" average diameters (Hendry 1976). In contrast, for olfactory vesicles the section was thick compared to the profile diameter (1.6 μm) and thus the "true" average diameter equals the average diameter of the profiles (Hendry 1976).

The average diameter of the openings of the ducts of the Bowman's glands was calculated in the following way. Seven ducts were identified for which serial sections were made through the entire opening. The central section was identified and the distance across the duct was measured. Six measurements were made for each duct from sections on either side of the central section.

Numbers of nuclei and olfactory vesicles

In estimating "true" cell numbers, the method of Abercrombie (1946) was applied:

$$Nc = N_A \left(\frac{T}{(T + D)} \right)$$

where Nc is the corrected number of nuclei whose centres lie in the volume of the section, N_A is the actual number of nuclear profiles counted in the area of the section, T is section thickness and D is the average diameter of cell nuclei. Calculation of Nc is subject to error due to overestimation of D because of the difficulty in discriminating the smallest nuclear segments within the underlying cytoplasm (Weibel 1980). In this case, errors in Nc were calculated to be less than 1%. In estimating the "true" number of olfactory vesicles, where T is about the same magnitude as D, small errors in estimating D could lead to relatively large errors in Nc. Therefore Nc was calculated using the iterative method of Hendry (1976) as it was devised specifically to overcome this problem.

The corrected numbers of cell nuclei and olfactory vesicles are now directly comparable as each represents the numbers whose centres lie in the plane of section. That is, the numbers whose centres lie beneath an epithelial surface area of 400 μm^2. (The sections were 2 μm thick and the field width was 200 μm along the epithelial surface.) Thus all numbers of nuclei and vesicles in the analysis presented below are those within this "unit surface area".

Epithelial thickness

The locations and types of cell nuclei and the outline of the epithelial section were stored on disk and drawn on a Hewlett

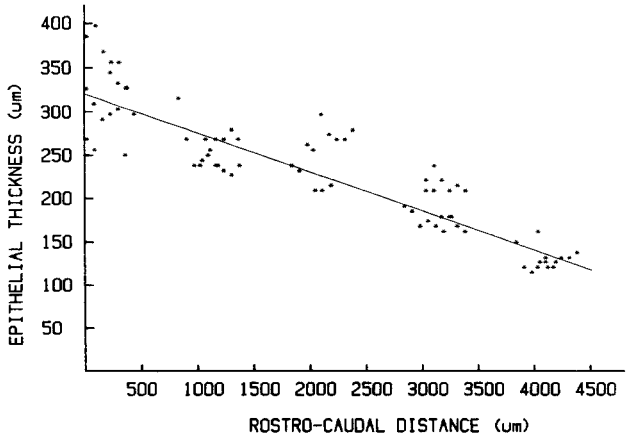

Fig. 1. The thickness of the olfactory epithelium decreases from rostral to caudal in the nasal cavity. In each animal a longitudinal strip of epithelium was transversely sectioned from the rostral to the caudal end. "Rostro-caudal distance" is the distance of each sampled section from the most rostral section

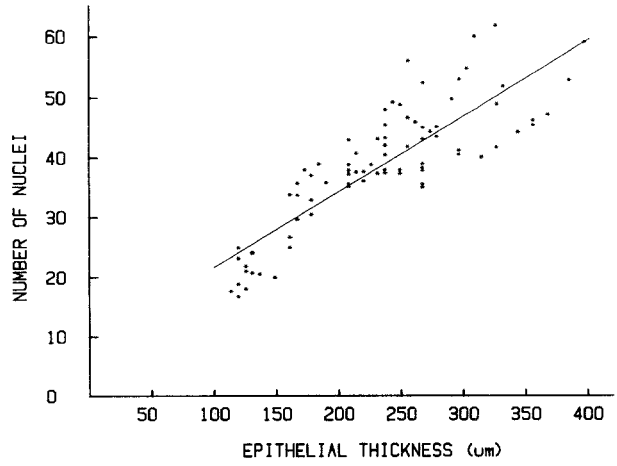

Fig. 2. The total number of cell nuclei increases with epithelial thickness. Each point represents the number of nuclei whose centres lie within the 2 μm section, from the epithelial surface to the basement membrane. Counts were made over a surface distance of 200 μm, so each point represents the number of nuclei beneath a surface area of 400 μm^2

Packard 7470A plotter at 160 × magnification. On each plot the thickness of the epithelium from the lumenal surface to the basement membrane was measured in the centre of the section.

Stastical analysis

Relations between the numbers of cell nuclei and olfactory vesicles, the total number of nuclei per section and epithelial thickness were analysed using linear and derivative-free non-linear regression (Dixon and Brown 1979). Various non-linear equations were fitted to the data. The equations considered to be the best fit between the variables were those with the smallest mean square error.

Results

Epithelial area

The mean area (± SEM) of the ventral surface of the nasal cavity was 26.01 ± 0.13 mm^2.

Regional variation in epithelial thickness

In all animals the epithelium was more thick rostrally than caudally (Fig. 1). A linear regression indicates a significant negative correlation between the thickness of the epithelium and the rostro-caudal sampling distance ($r = -0.90$, $p < 0.001$, $n = 81$. The linear component of the regression accounts for 80% of the variance.) The thickness of the epithelium was directly proportional to the total number of nuclei in each section (Fig. 2) ($r = 0.85$, $p < 0.001$, $n = 81$. The linear component of the regression accounts for 72.3% of the variance.)

Epithelial cell types

Typical sections through thick and thin epithelium are shown in Fig. 3a, b. The three main cell types were identified according to the following criteria. Supporting cell nuclei were identified by their superficial location, their elongate shape and dark nuclear staining with relatively few, dark spots of heterochromatin. Receptor cell nuclei were located below the supporting cell nuclei, and were more lightly stained, less elongate, with a different, blotchy heterochromatin pattern. Globose basal cell nuclei were cuboidal, lightly stained, with a less distinct heterochromatin pattern. Some cells classified as basal, showed obvious mitotic figures. Others, not counted, were darkly staining, non-cuboidal in shape.

It was usually easy to distinguish between the receptor and basal cell nuclei as the basal cell nuclei were more lightly staining. At times though, this distinction was difficult as there would be "transitional" nuclear types which had a light background stain typical of basal cells, combined with the dark, blotchy chromatin pattern of receptor cells. These cells were placed in either category depending on the dominance of one or other characteristic. There were various other cell nuclei in the epithelium which were not counted. Superficial to the supporting cell layer there were a few nuclei with a mixture of morphologies (Fig. 3a). Some of these looked pycnotic, some looked like receptor cell nuclei and others were probably nuclei from the ducts of Bowman's glands which penetrated the lumen out of the plane of

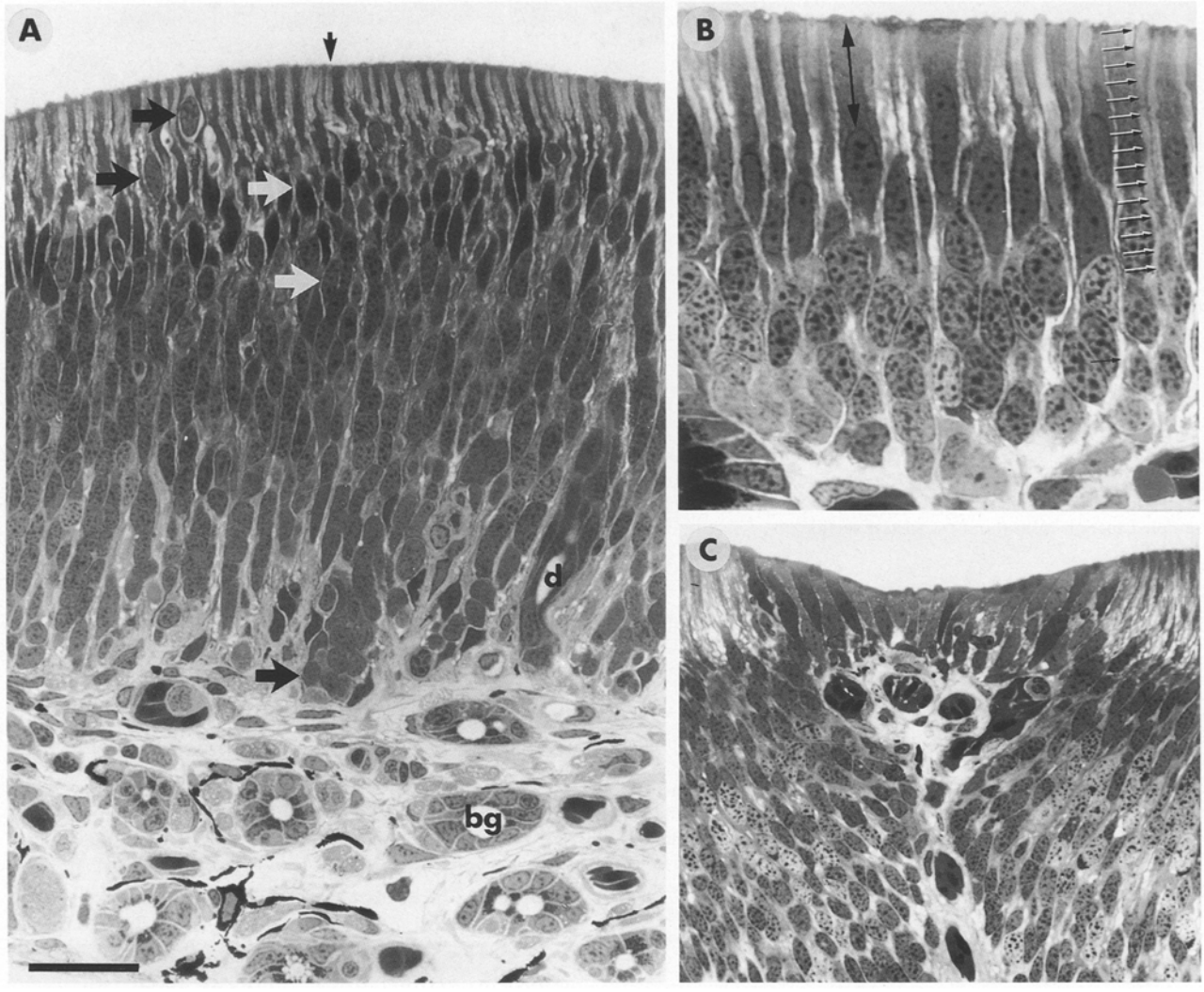

Fig. 3. A A section, stained with Toluidine blue, through rostrally located epithelium. Uppermost is the lumenal surface formed by the lightly stained olfactory vesicles (vertical arrow) and the darkly stained cytoplasm of supporting cells. The neuroepithelium is characterised by an obvious layering of nuclei of supporting cells (upper white arrow), receptor neurones (lower white arrow) and globose basal cells (lower black arrow) above the convoluted basement membrane. Other nuclei are also seen. Above the layer of supporting cell nuclei are nuclei which may be degenerating cells (upper black arrows). These were not included in the analysis and nor were the nuclei surrounding ducts (d) of Bowman's glands (bg). Bar = 40 μm. **B** A section through caudal epithelium. More obvious in this thin epithelium is the association between the dark cytoplasm at the surface and the supporting cell nucleus (double arrow). Flanking the supporting cells are the pale dendrites of receptor neurones which extend from the surface to the receptor cell nuclei (small arrows). Bar (in **A**) = 25 μm. **C** A section through the surface opening of a duct of a Bowman's gland showing the variety of nuclear types associated with this structure. None of these nuclei were included in the analysis. Bar (in **A**) = 50 μm

section. Periodically these ducts were in the plane of section but their nuclei were not counted. Usually these nuclei were fusiform and dark staining but sometimes they had other appearances (Fig. 3c). Generally, if the identity of a cell was in doubt, it was not counted. Olfactory vesicles were identified in these sections by their light staining, in contrast to the cytoplasm of the supporting cells which was much darker. This is seen best in sections of thin epithelium where the dark supporting cell cytoplasm can be traced from the nucleus to the lumenal surface adjacent to lighter staining dendritic processes which can be traced from the deeper receptor cell nuclei (Fig. 3b).

Morphometric analysis

Perhaps the most significant result of the morphometric analysis was the discovery that the density

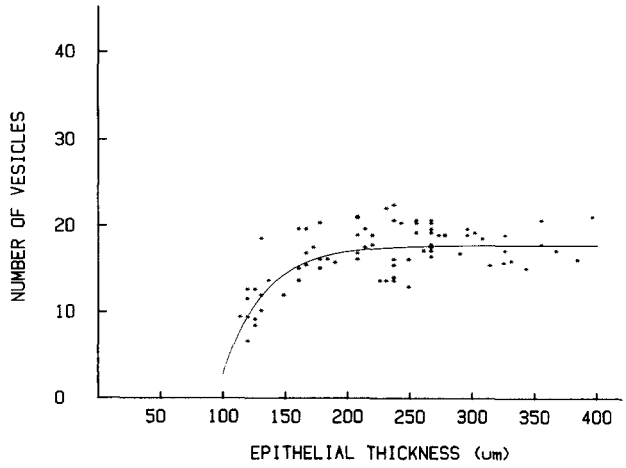

Fig. 4. The density of olfactory vesicles, representing mature receptor cells, is constant over most of the olfactory epithelium, regardless of epithelial thickness. Each point shows the number of vesicles in each section which represents an epithelial surface area of 400 μm^2. A non-linear regression fitted to the curve illustrated [$Y = 17.79\ (1\text{-}e^{-0.033(X-94.54)})$] had a mean square error = 5.49. For comparison a linear regression ($Y = 10.47 + 0.03X$, $r = 0.53$, $p < 0.001$) had a mean square error = 8.49

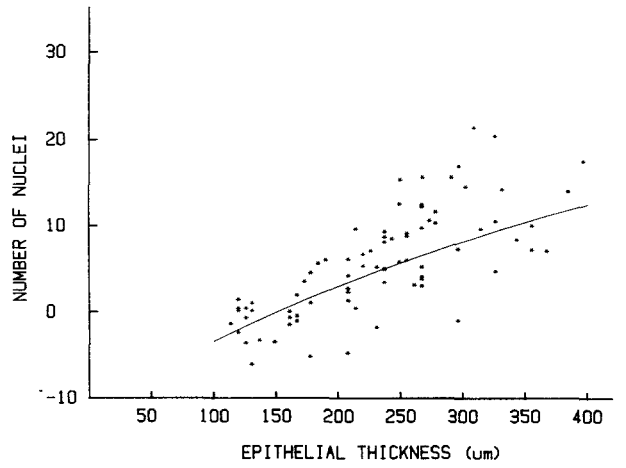

Fig. 6. The density of immature receptor cells increases with epithelial thickness. Each point is the subtraction of the number of olfactory vesicles per section (Fig. 4) from the total number of receptor cell nuclei per section (Fig. 5). A non-linear regression fitted to the curve illustrated [$Y = 31.84\ (1\text{-}e^{-0.002(X-150.83)})$] had a mean square error of 17.05. A linear regression ($Y = 9.62 + 0.65X$) fitted the data almost as well (mean square error = 17.08)

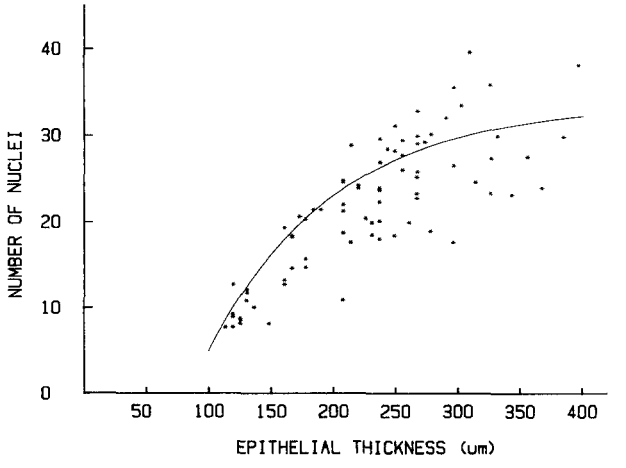

Fig. 5. The density of receptor cell nuclei increases with increasing epithelial thickness. Each point shows the number of nuclei in the receptor cell layer beneath an epithelial surface area of 400 μm^2. A non-linear regression fitted to the curve illustrated [$Y = 33.67\ (1\text{-}e^{-0.008(X-84.39)})$] had a mean square error = 17.23. For comparison, a linear regression ($Y = 0.85 + 0.09X$, $r = 0.81$, $p < 0.001$) had a mean square error = 21.23

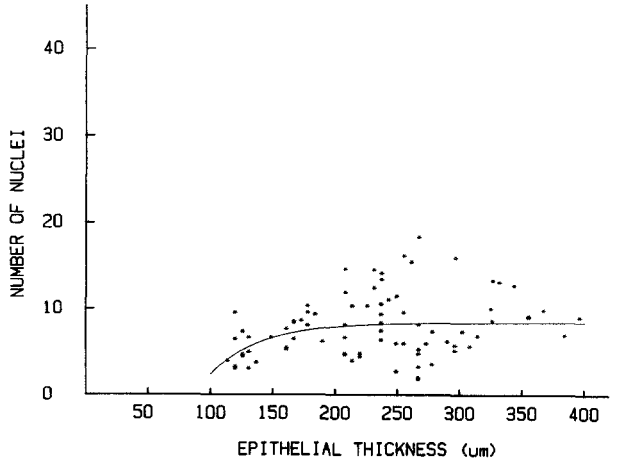

Fig. 7. The density of basal cells is constant over most of the olfactory epithelium, regardless of epithelial thickness. Each point shows the number of nuclei in the receptor cell layer beneath an epithelial surface area of 400 μm^2. A non-linear regression fitted to the curve illustrated [$Y = 8.43\ (1\text{-}e^{-0.024(X-86.21)})$] had a mean square error = 12.01. For comparison, a linear regression ($Y = 4.21 + 0.01X$, $r = 0.28$, $p = 0.01$) had a mean square error = 12.46)

of olfactory vesicles was constant over most of the epithelium (Fig. 4). Above a critical epithelial thickness of about 200 μm the olfactory vesicle density reached 18 vesicles within the "unit surface area" of 400 μm^2. This density can be expressed as 4.5×10^4 per mm^2. In contrast, the total number of receptor cell nuclei in each section was not constant, but increased with epithelial thickness (Fig. 5). Thus, except in the thinnest epithelium, there was a non-linear relation between olfactory vesicles, which represent mature receptor cells, and those nuclei classified histologically as receptor nuclei, which must actually represent both mature and immature receptor cells. Therefore, the number of immature receptor cells was calculated by subtracting the number of olfactory vesicles per section from the

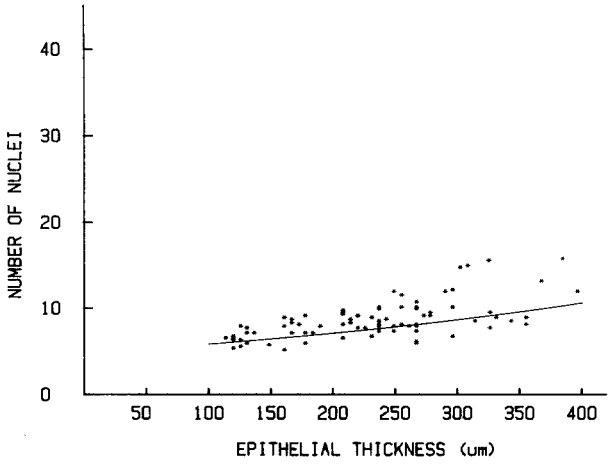

Fig. 8. The density of supporting cells increases slightly with increasing epithelial thickness. Each point shows the number of supporting cell nuclei beneath an epithelial surface area of 400 μm^2. A non-linear regression fitted to the curve illustrated ($Y = 4.77e^{0.002X}$) had a mean square error = 3.11. A linear regression ($Y = 3.75 + 0.020X$, $r = 0.62$, $p < 0.001$) fitted the data almost as well (mean square error = 3.13)

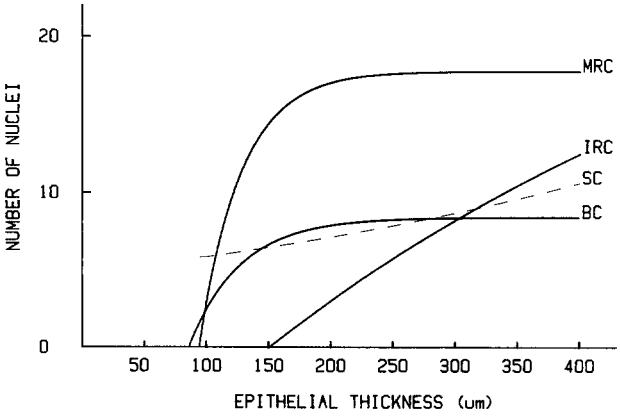

Fig. 9. A comparison of the densities of different cell types in olfactory epithelium of varying thickness. The curves are those in Figs. 4, 6–8. MRC = mature receptor cells. IRC = immature receptor cells. BC = basal cells. SC = supporting cells

total number of receptor nuclei per section (Fig. 6). The number of basal cell nuclei in each section was quite variable but like the mature receptor cells, the number of basal cell nuclei per section reached a constant level in epithelium above about 200 μm thick (Fig. 7).

In marked contrast to the other cell types, the numbers of supporting cells per section shows a very different trend with increasing epithelial thickness (Fig. 8). The density of supporting cell nuclei can be fitted almost equally well by a linear regression or an exponentially increasing function (see Fig. 8 caption), neither of which intersects the abscissa near the intersection of the other cell types (Fig. 9).

Table 1. Average diameters of profiles

Profile type	Mean diameter of profiles (μm ± SEM)	Corrected diameter of profiles (μm ± SEM)
Olfactory vesicle	1.64 ± 0.05 (n = 75)	1.64 ± 0.05
Lumenal surface of supporting cell	4.78 ± 0.65 (n = 870)	6.08 ± 0.83
Supporting cell nucleus	6.30 ± 0.13 (n = 91)	8.01 ± 0.16
Receptor cell nucleus	6.87 ± 0.07 (n = 305)	8.75 ± 0.09
Basal cell nucleus	7.67 ± 0.27 (n = 54)	9.76 ± 0.34

Table 1 presents the average profile diameters for the different nuclei, olfactory vesicles and the lumenal surface of supporting cells. The "corrected diameters" take into account the section thickness as described above. The average diameter of the openings to the ducts of the Bowman's glands was 147.28 ± 7.78. From these diameters the areas of epithelial surface occupied by an olfactory vesicle, a supporting cell and a Bowman's gland duct were calculated to be respectively, 2.11 μm^2, 29.08 μm^2 and 17,043 μm^2.

Discussion

By use of a morphometric analysis, this study has revealed major new insights into the organisation of the olfactory epithelium of the tiger salamander. Notably, the increase in epithelial thickness from caudal to rostral in the nasal cavity was not accompanied by an increase in the number of mature receptor neurones: above a critical epithelial thickness of about 200 μm the surface density of olfactory vesicles was constant and independent of epithelial thickness. Indeed the increase in epithelial thickness beyond 200 μm was almost entirely due to the accumulation of immature receptor cells. These observations indicate that the rate of neuronal differentiation, like the rate of basal cell mitosis, is inversely related to epithelial thickness.

It is concluded therefore that neurogenesis, the formation of mature olfactory receptor cells, must be a "regulated" rather than an "automatic" process. The present results indicate that one regulatory mechanism may act through the availability of space at the epithelial surface for newly developing dendrites.

Methodological considerations

As this study does not use electron microscopy, occasional errors may arise in the correct classifica-

tion of nuclei into particular cell classes. These errors have been reduced by the use of high resolution light microscopy and by a statistical treatment of the data. Our results are based on the observation of about 18,000 nuclear profiles and 1,800 olfactory vesicles in 80 epithelial sections. Such a study would be impractical with electron microscopy since the number of nuclear profiles whose centres lie in the plane of section reduces rapidly with section thickness. (For example, the number of 8 μm diameter nuclei whose centres lie within a 2 μm section is 8 times the number within a 0.2 μm section.)

In the olfactory epithelium the errors involved in assigning a nucleus into the three cell classes revolve around two main sources of confusion: supporting cell vs receptor cell, and receptor cell vs basal cell. In the former distinction the morphology, staining characteristics and epithelial position of the two cell types are sufficiently different that errors are unlikely except where the nuclear fragments are small. As the decision is dichotomous, those nuclei whose identity are confused will be assigned the wrong category 50% of the time so that over a large number of observations, false classifications of one cell type will equal false classifications of the other type. A similar process will occur at the epithelial interface between receptor cell and basal cell nuclei although the number of "confusing" nuclei is probably larger since there are transitional forms between "true" basal and "true" receptor cell nuclei. Therefore the basal/receptor cell dichotomy involves confusion both of nuclear fragments and of nuclei lying directly in the plane of section. This means that the classification of transitional forms as "basal" or "receptor" cell nuclei could arbitrarily inflate the numbers of either group depending on the bias of the observer. As the observer was the same for all counts this bias may mean that the curves for basal cells and immature receptor cells have been displaced up and down (or vice versa) from their "true" values. This remains a problem, even under electron microscopy, whenever a continuum of cell types is forced into a dichotomous classification. However, this problem does not detract from the fundamental observation that whilst nuclear numbers increase with epithelial thickness, the number of mature receptor neurones (indicated by olfactory vesicles) remains constant thereby resulting in an accumulation of immature cell types.

Morphology of the epithelial surface

Olfactory vesicle density was constant over most of the salamander olfactory epithelium. This "optimal" surface density of 4.5×10^4 per mm^2 was reached in epithelium that was at least 200 μm thick (Fig. 4), which represents approximately the rostral 2/3 of the ventral epithelium in these animals. Previous estimates of surface densities of olfactory vesicles vary markedly (for a recent review see: Menco 1983). The following are estimates for various species expressed as the number ($\times 10^4$) per mm^2: frog, 4.5 (Menco 1980), 8 (Getchell 1973); or 4.5–9.1 (Menco et al. 1978; Menco 1983); pig, 6.2 (Gasser 1956); rabbit, 12 (Allison and Warwick 1949), 15 (Clark and Warwick 1946); and rat, 8.3 (Menco 1980), 5–10 (Hinds and McNelly 1981). Some authors report gender and age differences in surface densities (Hinds and McNelly 1981; Menco 1980, 1983), differences in estimates according to histological procedure (Menco et al. 1978; Menco 1983), as well as differences in estimates from different epithelial regions (Allison and Warwick 1949; Menco 1983). It is therefore difficult to make realistic conclusions about species differences. Furthermore, not all these studies account for section thickness and olfactory vesicle diameter in the calculations of surface density. These factors greatly affect the estimates of "true" numbers of items counted (Hendry 1976; Weibel 1980). For example, if these factors were not considered in the present study the "optimum" surface density of olfactory receptors would be 10.2×10^4 per mm^2.

It is now possible to construct a model of the surface of the olfactory epithelium of the tiger salamander. Obviously this surface is covered by olfactory vesicles, the lumenal surfaces of supporting cells and the openings of the ducts of Bowman's glands. Given their density (4.5×10^4 per mm^2) and the average area (2.11 μm^2), the olfactory vesicles occupy 95,000 μm^2 in each mm^2. The average area of lumenal surface occupied by a supporting cell is 29.08 μm and from Fig. 9 the median density of these cells is 8 per 400 μm^2 or 2×10^4 per mm^2. Therefore the supporting cells occupy 581,600 μm^2 in each mm^2. This leaves 323,400 μm^2 which is occupied by the duct openings. Each duct covered an average of 17,043 μm^2, therefore the density of the duct openings is 19 per mm^2. This density can be achieved in a hexagonal array where each duct is equidistant (248 μm) from six others. The supporting cells are distributed between the ducts, possibly also in a hexagonal array, with olfactory vesicles distributed in interconnecting rings surrounding the supporting cells (Graziadei and Monti Graziadei 1976) and sometimes even enclosed within the supporting cells (Breipohl et al. 1974).

The ventral epithelium has an average area of 26 mm^2. The olfactory vesicle density was 4.5×10^4 per mm^2, giving the total number of mature olfactory receptor neurons of about 1.2 million. The dorsal

olfactory epithelium is slightly smaller than the ventral epithelium (Breipohl et al. 1982), and therefore the total number of mature receptor neurons on each side of the nose would be in the range of 2 million, in animals weighing only 50 g. For comparison, the adult rabbit is estimated to have 50 million mature receptors in each side of the nose (Allison and Warwick 1949).

Regional differences in neuronal maturation

Although the number of mature receptor cells reaches a constant level in epithelium at least 200 μm thick, the number of immature receptor cells continues to increase with epithelial thickness (Fig. 9). In the thinnest epithelium there are only basal and mature receptor cells whose numbers increase rapidly as epithelial thickness increases. When the epithelium reaches 150 μm thick the numbers of mature receptor cells and basal cells have almost reached constant levels and the further increase in cell numbers is contributed almost entirely by immature receptor cell nuclei. This leads us to suggest that the limit to maturation of receptor cells may be the availability of dendritic space at the surface of the epithelium. In other words, once the surface density of olfactory vesicles reaches 4.5×10^4 per mm^2 the final maturation of developing receptor cells is prevented. This would lead to an accumulation of "almost mature" receptor cells, waiting for a dendritic vacancy at the epithelial surface. This may not be unique to the tiger salamander as there is evidence from a freeze-fracture study of rat olfactory epithelium that the density of dendrites just below the surface was over twice the density of olfactory vesicles on the surface (Menco 1980).

The accumulation of immature receptor cells can also be interpreted as evidence that the rate of development and differentiation from basal to mature receptor cells may be slower on average in the thick, rostral epithelium compared to the thinner, caudal epithelium. This parallels rostro-caudal differences in the uptake of ^{3}H-thymidine by the basal cells in this tissue. The rostral olfactory epithelium is up to 3 times as thick as the caudal epithelium yet after an injection of ^{3}H-thymidine the thinner, caudal epithelium may have 3 times the number of labelled basal cell nuclei (Mackay-Sim and Patel 1984). That is, the thinner epithelium may have 100 cells per field, 10 of which are labelled, whilst the same field-width of thicker epithelium may have only 3 labelled nuclei out of 300 cells. It follows, therefore that there must be a rostro-caudal difference in the rate of mitosis, expressed either as a difference in the duration of the cell generation cycle or a difference in the relative number of mitotically active cells. Estimates based on the number of mitoses per 1000 basal cells also indicate rostro-caudal differences in the olfactory epithelium of young and adult mice (Breipohl et al. 1985b).

The regional differences in neuronal maturation observed in this study add further to previously reported rostro-caudal variations in olfactory receptor cell physiology in this species (Mackay-Sim and Kubie 1981). First, rostral epithelium was less responsive to odorants than caudal epithelium (Mackay-Sim et al. 1982; Mackay-Sim and Shaman 1984). Second, rostral epithelium responded to individual odorants differently from caudal epithelium (Kubei et al. 1980; Nathan and Moulton 1981; Mackay-Sim et al. 1982; Mackay-Sim and Shaman 1984). Finally, rostral epithelium projects to dorsal olfactory bulb whilst caudal epithelium projects ventrally (Mackay-Sim and Nathan 1984). It is quite possible that the regional differences in neuronal development observed in the present study may contribute to the differences in physiology of the mature receptor cells.

Supporting cells

In each unit surface area of the epithelium the numbers of supporting cell nuclei increase only slightly with epithelial thickness and do not drop toward zero in the thinnest epithelium, contrary to the other cell types (Fig. 9). Presumably in the thinnest epithelium, some minimum number of supporting cells would be required to maintain the integrity of the epithelial surface, a function of supporting cells implied by the presence of tight junctions around their apical perimeters (Breipohl et al. 1974; Kerjaschki and Hörandner 1976; Menco 1980). The small rostral increase in supporting cell numbers probably reflects their function in providing a physical structure for the increasing numbers of other epithelial elements (Allison 1953; Breipohl et al. 1974; Graziadei and Monti Graziadei 1976).

Like receptor cells, supporting cells also appear to be replaced. In studies using ^{3}H-thymidine a few nuclei in the supporting cell layer are labelled soon after injection, simultaneous to labelling of nuclei along the basement membrane (Moulton et al. 1970; Graziadei and Metcalf 1971; Graziadei and Monti Graziadei 1979; Mackay-Sim and Patel 1984). Mitotic figures have been observed among the supporting cell nuclei, though much more rarely than in the basal cell layer (Graziadei and Monti Graziadei 1979; Moulton 1975). The most parsimonious explanation for these observations is that supporting cells are

replaced through division of cells within the supporting cell layer (Breipohl et al. 1973; Graziadei and Monti Graziadei 1978; Mackay-Sim and Patel 1984). Earlier suggestions were that mitosis in the supporting cell layer is secondary to a supply of daughter cells from basal cell mitosis (Graziadei and Metcalf 1971; Moulton et al. 1970; Moulton 1975). The present study indicates that this is unlikely because the numbers of supporting cells behave quite differently from all the other cell types within the epithelium. Theoretically at least, basal cell and other cell numbers drop to zero, leaving only supporting cells within the epithelium (Fig. 9). Therefore the numbers of supporting cells are quite independent of the presence of basal cells, and so basal cell mitosis is unlikely to give rise to new supporting cells.

Neurogenesis and receptor cell turnover

With the present results the process of neurogenesis and receptor cell turnover can be viewed from a new perspective. Since there are regional variations in the numbers of immature receptor cells and in the uptake of ^{3}H-thymidine by basal cells (Mackay-Sim and Patel 1984), it follows that neurogenesis and receptor cell development can vary throughout the olfactory epithelium. Our results thus support a model in which there may be multiple mechanisms of control over these processes (for a review see Breipohl et al. 1986). One phenomenon suggested by the constant surface density of olfactory vesicles is that a physical or chemical mechanism exists which prevents the final maturation of "almost mature" cells until dendritic space becomes available. This mechanism may act locally to control the development and survival of "almost mature" cells which may die after some period if they cannot find dendritic space at the surface. Hinds and others (1984) have proposed that mature receptor cells may live for very long periods until disease or other external factors cause their death. They have suggested also that newly developing receptor cells may die if they do not find synaptic space at the olfactory bulb. Therefore the neurogenic process could be viewed as a mechanism to provide a continual supply of "almost mature" neurons should they be required. However, synaptic connections with the bulb and dendritic projections to the epithelial surface would remain intact indefinitely, until a mature receptor cell died. At this time it would be replaced very rapidly as there would be an "almost mature" cell located locally, with its dendrite just below the epithelial surface and its axon perhaps already grown to the olfactory bulb.

Acknowledgements. The authors gratefully acknowledge financial support from the following grants: NHMRC 850400, ABF 8285 to A.M-S; and DFG Br 358/5-2, BRF 52, NHMRC 860587 to W.B.

References

Abercrombie M (1946) Estimation of nuclear population from microtome sections. Anat Rec 94: 274–329

Allison AC (1953) The morphology of the olfactory system in vertebrates. Biol Rev 28: 195–244

Allison AC, Warwick RTT (1949) Quantitative observations on the olfactory system of the rabbit. Brain 72: 187–197

Breipohl W, Grandt D, Rehn B, Mackay-Sim A, Hierche H (1985a) Investigations of cell replacement in the olfactory epithelium. Neurosci Lett Suppl 19: S7

Breipohl W, Laugwitz HJ, Bornfeld N (1974) Topological relations between the dendrites of olfactory sensory cells and sustentacular cells in different vertebrates. J Anat 117: 89–94

Breipohl W, Mackay-Sim A, Grandt D, Rehn B, Darrelmann C (1986) Neurogenesis in the vertebrate main olfactory epithelium. In: Breipohl W (ed) Ontogeny of olfaction. Springer, New York, pp 21–34

Breipohl W, Mestres P, Meller K (1973) Licht- und elektronmikroskopische Befunde zur Differenzierung des Riechepithels der weißen Maus. Verh Anat Ges 67: 443–449

Breipohl W, Moulton DG, Ummels M, Matulionis D (1982) Spatial pattern of sensory cell terminals in the olfactory sac of the tiger salamander. I. A scanning electron microscope study. J Anat 134: 757–769

Breipohl W, Rehn B, Molyneux GS, Grandt D (1985b) Plasticity of neuronal cell replacement in the main olfactory epithelium of mouse. Proc XII Int Anat Congr London

Clark WE, Le Gros, Warwick RTT (1956) The pattern of olfactory innervation. J Neurol Neurosurg Psychiat 36: 33–45

Dixon WJ, Brown MB (1979) BMDP Biomedical Computer Programs P-series. University of California Press, Berkeley

Gasser HS (1956) Olfactory nerve fibres. J Gen Physiol 39: 473–498

Getchell TV (1973) Analysis of unitary spikes recorded extracellularly from frog olfactory receptor cells and axons. J Physiol 234: 533–551

Graziadei PPC, Metcalf JF (1971) Autoradiographic and ultrastructural observations on the frog's olfactory mucosa. Z Zellforsch 116: 305–318

Graziadei PPC, Monti Graziadei GA (1976) Olfactory epithelium of *Necturus maculosus* and *Ambystoma tigrinum*. J Neurocytol 5: 11–32

Graziadei PPC, Monti Graziadei GA (1978) Continuous nerve cell renewal in the olfactory system. In: Jacobson M (ed) Development of sensory systems. Springer, Berlin, pp 55–84

Graziadei PPC, Monti Graziadei GA (1979) Neurogenesis and neuron regeneration in the olfactory system of mammals. I. Morphological aspects of differentiation and structural organization of the olfactory sensory neurons. J Neurocytol 8: 1–18

Halasz P, Martin PR (1984) A microcomputer based system for semiautomatic analysis of histological sections. Proc R Microscop Soc 19: 312P

Hendry IA (1976) A method to correct adequately for the change in neuronal size when estimating neuronal numbers after nerve growth factor treatment. J Neurocytol 5: 337–349

Hinds JW, McNelly NA (1981) Aging in the rat olfactory system: correlation of changes in the olfactory epithelium and olfactory bulb. J Comp Neurol 203: 441–453

Hinds JW, Hinds PL, McNelly NA (1984) An autoradiographic study of the mouse olfactory epithelium: evidence for long-lived receptors. Anat Rec 210: 375–383

Kerjaschki D, Hörandner H (1976) The development of mouse olfactory vesicles and their cell contacts: a freeze etching study. J Ultrastruct Res 54: 420–444

Kubie J, Mackay-Sim A, Moulton DG (1980) Inherent spatial patterning of responses to odorants in the salamander olfactory epithelium. In: van der Starre H (ed) Olfaction and taste, Vol VII. IRL Press, London, pp 163–166

Mackay-Sim A, Beard MD (1987) Hypothyroidism disrupts neural development in the olfactory epithelium of adult mice. Dev Brain Res 36: 190–198

Mackay-Sim A, Kubie JL (1981) The salamander nose: a model system for the study of spatial coding of olfactory quality. Chem Senses 6: 249–257

Mackay-Sim A, Nathan MH (1984) The projection from the olfactory epithelium to the olfactory bulb in the salamander, *Ambystoma tigrinum*. Anat Embryol 170: 93–97

Mackay-Sim A, Patel U (1984) Regional differences in cell density and cell genesis in the olfactory epithelium of the salamander, *Ambystoma tigrinum*. Exp Brain Res 57: 99–106

Mackay-Sim A, Shaman P (1984) Topographic coding of odorant quality is maintained at different concentrations in the salamander olfactory epithelium. Brain Res 297: 207–217

Mackay-Sim A, Shaman P, Moulton DG (1982) Topographic coding of olfactory quality: patterns of epithelial responsivity in the salamander. J Neurophysiol 48: 584–596

Menco BPM (1980) Qualitative and quantitative freeze-fracture studies on olfactory and nasal respiratory structures of frog, ox, rat and dog. I. A general survey. Cell Tiss Res 207: 183–209

Menco BPM (1983) The ultrastructure of olfactory and nasal respiratory epithelium surfaces. In: Reznik G, Stinson SF (eds) Nasal tumors in animals and man, Vol 1. Anatomy, physiology and epidemiology. CRC Press, Boca Raton Florida, pp 45–102

Menco BPM, Leunisson JLM, Bannister LH, Dodd GH (1978) Bovine olfactory and nasal epithelium surfaces. Cell Tiss Res 193: 503–524

Moulton DG (1975) Cell renewal in the olfactory epithelium of the mouse. In: Denton DA, Coughlan JP (eds) Olfaction and taste Vol V. Academic Press, New York, pp 111–114

Moulton DG, Celebi G, Fink RP (1970) Olfaction in mammals – two aspects: proliferation of cells in the olfactory epithelium and sensitivity to odours. In: Wolstenholme GEW, Knight J (eds) Taste and smell in vertebrates. Churchill, London, pp 227–250

Nathan MH, Moulton DG (1981) 2-deoxyglucose analysis of odorant-related activity in the salamander olfactory epithelium. Chem Senses 6: 259–266

Weibel ER (1980) Stereological methods, Vol 2. Theoretical foundations. Academic Press, London

Received August 7, 1987 / Accepted October 28, 1987